Polymer 49 (2008) 2947–2956

Contents lists available at ScienceDirect

Polymer

journal homepage: www.elsevier.com/locate/polymer

Morphology, thermal stability and rheology of poly(propylene carbonate)/organoclay nanocomposites with different pillaring agents

Zhihao Zhang [a,b,c,d], Joong-Hee Lee [a,*], Seung-Hee Lee [a], Seok-Bong Heo [a], Charles U. Pittman, Jr [d,**]

[a] Polymer BIN Fusion Research Team, School of Advanced Materials Engineering, Chonbuk National University, Jeonju, Jeonbuk 561-756, Republic of Korea
[b] State Key Laboratory of Polymer Physics and Chemistry, Changchun Institute of Applied Chemistry, Chinese Academy of Sciences, Changchun, Jilin 130022, PR China
[c] Institute for Combustion Science and Environmental Technology, Western Kentucky University, Bowling Green, KY 42101, USA
[d] Department of Chemistry, Mississippi State University, Mississippi State, MS 39762, USA

ARTICLE INFO

Article history:
Received 20 February 2008
Received in revised form 7 April 2008
Accepted 11 April 2008
Available online 25 April 2008

Keywords:
Poly(propylene carbonate)
Organoclay
Nanocomposite

ABSTRACT

Unpillared montmorillonite PGV and five organoclays (Nanocor's Nanomer I.44P, I.24TL and I.34TCN and Southern Clay Product's C25A and C30B) were high shear melt-blended (2.5 wt%) into poly(propylene carbonate) (PPC). Solubility parameters of the clay pillaring agents versus that of PPC were used to predict clay/PPC miscibilities and these were compared to XRD and TEM nanoclay dispersion measurements. Clays I.34TCN and C30B, with the highest predicted pillaring agent/PPC miscibilites, had partially exfoliated morphologies. Clays I.24TL, C25A and I.44P, with pillaring agents predicted to be less PPC miscible, were less highly nanodispersed. Quaternary ammonium pillars with two 2-hydroxyethyl groups promoted the best nanodispersion in PPC. 12-Aminododecanoic acid (in I.24TL) promoted the intercalation. Dimethyl dialkyl quaternary ammoniums (in I.44P and C25A) were less effective. Organoclay dispersion improved the thermal stability. The PPC/I.24TL nanocomposite, with the most stable 12-aminododecanoic acid pillar, was the most thermally stable (PPC/I.34TCN and PPC/C30B were the second and third). The nanocomposites exhibited narrower linear viscoelastic zones than PPC and solid-like behaviors in these linear zones.

1. Introduction

Poly(propylene carbonate) (PPC) is a thermoplastic prepared by polymerization of CO_2 with propylene oxide [1,2]. It possesses excellent adhesion to cellulosic substrates and improved lubricity [3] so that it has been used in binders [4], brazing pastes [5] and solutions [6], propellants [7] and diamond cutting tools [8]. Moreover, PPC is enzyme degradable [9], biocompatible [10] and readily processible [11]. It can also completely combust to produce only non-toxic carbon dioxide and water [3]. However, PPC has a poor thermal stability. This has prevented more extensive PPC use.

Polymer/clay nanocomposites often provide significant mechanical, thermal and physicochemical property improvements at small (0.5–5 wt%) clay loadings versus the pristine polymer or conventional clay-filled composites (micro- and macrocomposites) [12–16]. The hydrophilic clay platelet surfaces must have their natural interstitial metal cations (K^+, Na^+, Li^+, Mg^{2+}, Ca^{2+}, etc.) exchanged with organic cationic modifiers to make the galleries more organophilic and to enhance the *d*-spacings, while simultaneously reducing the attractive force between the platelets. A polymer may then intercalate more readily and further expand the *d*-spacings, leading to more efficient particle cleavage, platelet to small tactoid cleavage, platelet exfoliation and improved clay dispersion into the polymer at the nanometer scale. The use of PPC/organoclay nanocomposites provides a potential low cost method of extending the applications of PPC.

The organoclay pillaring agents' functional groups can be designed to interact or even chemically react with the continuous phase matrix polymer to improve the clay dispersion in matrix polymer. The pillaring agents used in this study, **1**–**5**, are shown in Fig. 1. Hydroxyethyl groups in such quaternary ammonium pillaring agents as **3** (in I.34TCN) and **5** (in Cloisite 30B, e.g. C30B) are frequently used. However, carboxyl groups present in modifier 12-aminododecanoic acid, e.g. **2** in Nanomer I.24TL, have seldom been investigated [17,18]. The effects of 12-aminododecanoic acid on polymer/I.24TL nanocomposite properties might be beneficial where the carbonyl-containing functions of polyesters or polycarbonates are present in the matrix.

Only a few papers exist on PPC/organoclay nanocomposites. Xu et al. reported that PPC/Cloisite 20A, pillared by dimethyl

* Corresponding author. Tel.: +82 63 270 2342; fax: +82 63 270 2341.
** Corresponding author. Tel.: +1 662 325 7616; fax: +1 662 325 7611.
E-mail addresses: jhl@chonbuk.ac.kr (J.-H. Lee), cpittman@chemistry.msstate.edu (C.U. Pittman, Jr.).

0032-3861/$ – see front matter © 2008 Elsevier Ltd. All rights reserved.
doi:10.1016/j.polymer.2008.04.034

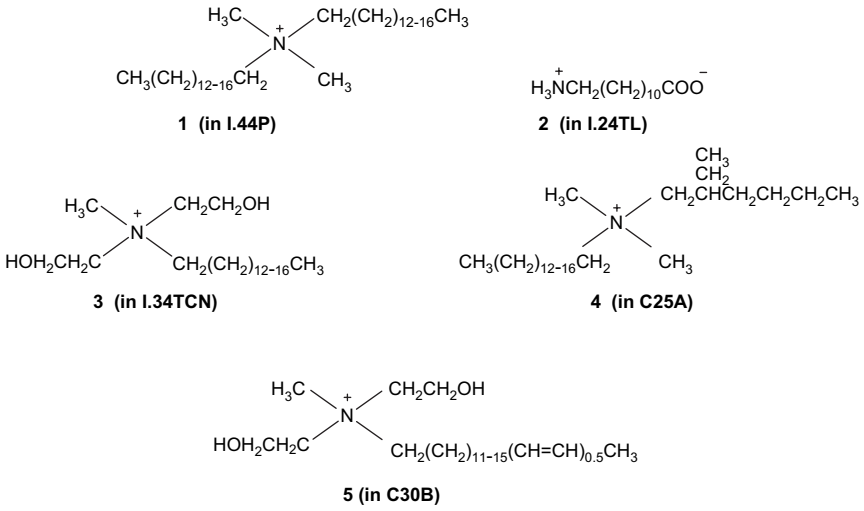

Fig. 1. Molecular structures of the pillaring agents used in this research (the clay identities, which contain these pillaring agents, are given in parentheses and the letter C stands for Cloisite).

dihydrogenated tallow ammonium ions, formed intercalated morphology nanocomposites [19]. Zhang et al. prepared partially delaminated and intercalated nanocomposites from maleated PPC (PPC-MA) with C30B and C20A, respectively [20]. They confirmed partial delamination mechanism of C30B in PPC-MA via XRD and FTIR [20]. The relationships among the PPC–organoclay miscibilities, clay dispersion in the nanocomposites and nanocomposite properties have not been clarified. PPC/organoclay nanocomposite rheology has never been reported.

In this contribution, PPC/organoclay nanocomposites were prepared with 2.5 wt% clay loadings via high shear melt-compounding. Organoclays, with various pillaring agents shown in Fig. 1 are identified by the acronyms used by the suppliers (viz. Nanomer I.44P, I.24TL and I.34TCN, and Cloisites C25A and C30B), and the unpillared inorganic clay PGV, with Na^+ counterions in the galleries, were used. The solubility parameters, δ, of pillaring agents **1**–**5** (Fig. 1) and PPC were calculated from their molecular structures using group contribution method of Van Krevelen [21]. The miscibilities between the PPC and each of the organoclays were predicted based on the absolute values of solubility parameter differences between PPC and the pillaring agent $|\delta_{PPC} - \delta_{modifier}|$. The effects of these predicated miscibilities on organoclay dispersion in PPC/organoclay nanocomposites, the composites' thermal stability and their rheology were investigated.

2. Experimental

2.1. Materials

PPC was obtained from Empower Materials Inc, with a polydispersity of 2.58, $M_w = 2.21 \times 10^5$ and $M_n = 8.57 \times 10^4$. The commercial organoclays, Nanomer I.44P, I.24TL and I.34TCN and polymer grade montmorillonite PGV, were obtained from Nanocor, Inc. Cloisite 25A (C25A) and 30B (C30B) were purchased from Southern Clay Products, Inc. These organoclays are natural montmorillonites modified, respectively, by pillaring agents **1**–**5** (Fig. 1) which were exchanged from their halide or methyl sulfate salts with clays. Agent **1** is the dimethyl dialkyl (alkyl: 70% C_{18}, 26% C_{16} and 4% C_{14}) ammonium cation, **2** is 12-aminododecanoic acid and **3** is the methyl bis-(2-hydroxyethyl) hydrogenated tallow (tallow: 65% C_{18}, 30% C_{16} and 5% C_{14}) ammonium cation. Modifier **4** is the dimethyl 2-ethylhexyl hydrogenated tallow ammonium cation and **5** is the methyl bis-(2-hydroxyethyl) tallow ammonium cation.

2.2. Composite preparation

The inorganic PGV clay and the organoclays were dried for 12 h under vacuum at 100 and 80 °C, respectively. PPC was dried for 24 h under vacuum at 60 °C and melted in a Haake Rheomix 600 high shear mixer at 160 °C with a 60 rpm blade speed for 2 min, using roller rotors in the mixer. The well-dried inorganic clay or organoclay was then added to give a 2.5 wt% loading and blended at 60 rpm with molten PPC at 160 °C for another 10 min. These blends were each prepared on a 50 g scale.

2.3. Estimation of the solubility parameters

The solubility parameter of homopolymer PPC or compound, e.g. pillaring agent **2**, was estimated using the group contribution method of Van Krevelen summarized previously [21]:

$$\delta_i = \frac{\sum_j F_j}{\sum_j V_j} \quad (1)$$

where F_j is the molar attraction constant of group j according to Van Krevelen and V_j is the molar volume of group j according to Fedors as described before [21].

Each of the pillaring agents **1**, **3**–**5** is actually a mixture with various hydrocarbon chains. For a compound mixture, Eq. (1) is modified as:

$$\delta_i = \frac{\sum_k F_k X_k}{\sum_k V_k X_k} \quad (2)$$

where F_k and V_k of group k possess the same meanings as those of F_j and V_j of the group j. X_k is the fraction of group k in the mixture.

The F_k and V_k values for the NH_2 group in **2** are 0 and 19.2, respectively. Both of these values for NH_4^+ ion in **1**, **3**–**5** were regarded as 0. The corresponding values for the OH group, attached to N^+ by the $-CH_2CH_2OH$ linkage in **3** and **5**, were 754 and 13.0 cm^3/mol, respectively [21].

2.4. Characterization

The X-ray diffraction (XRD) patterns were obtained on a Rigaku D/Max 2500PC X-ray diffractometer operated at 40 kV and 100 mA,

employing Cu $K\alpha_1$ radiation ($\lambda = 0.15406$ nm). Measurements were carried out in a fixed time mode with a 2 s step time and a step width of 0.02°.

A Philips Teccnai 20 transmission electron microscope (TEM) was used, employing a 120 kV accelerating voltage. Ultrathin composite slices (70 nm thick) were microtomed using a Leica EFMCS cryo-ultramicrotome.

Thermogravimetric analyses (TGAs) were carried out with a TA Instrumental Q50 TGA from 30 to 800 °C at a 10 °C/min heating rate in a dynamic nitrogen atmosphere.

Rheological measurements were performed at 140 °C using a Paar-Physica MCR 300 rheometer with a parallel plate geometry and 25 mm plate diameters. Dynamic amplitude sweeps from 0.1 to 100% strains at a 1 rad/s frequency were executed to determine the linear viscoelasticity range. Then dynamic frequency sweeps were performed from 0.05 to 100 rad/s at a small strain of 1% within the linear viscoelastic zone.

3. Results and discussion

3.1. Solubility parameters

The solubility parameter, δ, has been used to predict and explain the miscibility in multiple phase systems [22]. Calculations of δ are based on group contributions [21] and they have been applied previously to several polymer/pillaring agent miscibility evaluations [22–24]. If the clay pillaring agent's δ value is close to that of the polymer and the absolute value of the difference between them ($|\delta_{polymer} - \delta_{modifier}|$) is small, the miscibility is predicted to be good.

The PPC and pillaring agent δ values, calculated using the group contribution method of Van Krevelen [21], are given in Table 1. The δ values of **1**–**3** were calculated for the first time in this work since they were not available. Tallow T is a complex mixture containing both saturated and unsaturated hydrocarbon chains, where the unsaturated chains can have one or two double bonds. The hydrocarbon percent distributions within T and hydrogenated tallow HT [25] are listed in Table 2. The pillaring agent δ values fall into two distinct groups. Smaller δ values belong to the pillaring agents in organoclays I.24TL, I.44P and C25A, respectively (16.60, 16.41 and 16.10). Those of **3** (in I.34TCN) and **5** (in C30B) have significantly larger values of 19.14 and 19.12, respectively. These are much closer to PPC's δ value (22.76), predicting higher miscibilities with PPC. The $|\delta_{PPC} - \delta_{modifier}|$ values (Table 1) predict that PPC/I.34TCN and PPC/C30B nanocomposites would be more thoroughly nanodispersed than the PPC/I.24TL, PPC/I.44P and PPC/C25A systems when prepared under identical mixing conditions. This study experimentally (XRD and TEM) demonstrated that PPC/I.34TCN and PPC/C30B were, indeed, the most highly nanodispersed composites, while clays I.24TL, I.44P and C25A were less thoroughly nanodispersed when melt-blended identically. Thus, $\Delta\delta$ values, when significantly different, appear to be useful predictors of clay dispersion in PPC.

Table 1
Solubility parameters of the PPC and pillaring agents **1**–**5** in the organoclays and absolute values of the differences between them[a]

	PPC	**3** (in I.34TCN)	**5** (in 30B)	**2** (in I.24TL)	**1** (in I.44P)	**4** (in 25A)
δ ($J^{1/2}/cm^{3/2}$)	22.76	19.14	19.12	16.60	16.41	16.10
$\lvert\delta_{PPC} - \delta_{modifier}\rvert$ ($J^{1/2}/cm^{3/2}$)	–	3.62	3.64	6.16	6.35	6.66

[a] The structures of pillaring agents **1**–**5** are shown in Fig. 1.

Table 2
Hydrocarbon percent distributions in T and HT

		C20 (%)	C18 (%)	C17 (%)	C16 (%)	C15 (%)	C14 (%)
T	C–C bond		19.4	2.5	25.3	0.5	3.5
	One C=C bond	0.5	40.8		4.0		1.0
	Two C=C bonds		2.5				
HT	C–C bond		61.0	1.0	31.0	0.5	3.5
	One C=C bond		3.0				

3.2. X-ray diffraction

Intensity loss and disappearance of the clay's XRD base diffraction peak have often been used to indicate that delamination is occurring. However, Gilman et al. have pointed out that XRD analysis alone can lead to false interpretations of the extent of exfoliation [26,27]. Thus, XRD should be applied jointly with TEM analyses.

The XRD patterns of the pristine PPC, the dried starting clays and the PPC/clay nanocomposites are displayed in Fig. 2. Table 3 summarizes the *d*-spacings, intensities, and both the relative *d*-spacing and the intensity changes (of the clays in the composites versus the starting clays) from the XRD results. PPC exhibited a broad amorphous diffraction peak at 19.62° (inset of Fig. 2a). The PPC curve slanted upward from 2 to 10°. The *d*-spacing of the (001) plane, d_{001}, of unpillared PGV clay was 1.22 nm. The (001) diffraction peak of the PPC/PGV composite appeared as a very weak shoulder, due to the small clay volume fraction. No peak position shift was observed compared to PGV, revealing that the PPC had not intercalated into the clay galleries and its *d*-spacing did not change. This is consistent with immiscibility between PPC and PGV. PGV is poorly nanodispersed according to XRD analysis. Furthermore, TEM observations show that PPC/PGV was not a nanocomposite. All of the as-received pillared organoclays exhibited *d*-spacings significantly larger than that of unpillared PGV. The *d*-spacings of these organoclays and their PPC nanocomposites are now discussed.

The PPC/I.44P nanocomposite's d_{001} value (3.68 nm) and the *d*-spacing value of the (002) plane, d_{002} (1.83 nm), increased, compared to 2.57 and 1.28 nm, respectively, for as-received I.44P (Fig. 2b). This *d*-spacing expansion is consistent with a PPC/I.44P nanocomposite intercalated structure.

As-received C25A clay exhibited a (001) diffraction peak consistent with a *d*-spacing of 1.93 nm. The d_{001} value of the PPC/C25A nanocomposite increased to 3.37 nm and the smaller diffraction peak of the (002) plane emerged at a larger 5.26° angle (1.68 nm *d*-spacing) (Fig. 2c). The presence of a (002) plane diffraction peak was previously rationalized [28] by hypothesizing that the polymer extracted pillaring agent from a portion of the galleries during melt-compounding, resulting in the interlayer distances of the nanocomposite being slightly smaller than those of the organoclay. This would result in the loss of pillaring agent without polymer infusion into the galleries. The relative *d*-spacings and intensities of the clays and their PPC nanocomposites are shown in Table 3 where the superscript 0 refers to the starting clay values. The relative *d*-spacing increase, $\Delta d_{001}/d^0_{001}$, and the relative decrease in peak intensity $-\Delta I_{001}/I^0_{001}$, of the PPC/C25A nanocomposite were larger than those of the PPC/I.44P nanocomposite, respectively (Table 3). This suggests that the dispersion of C25A in the nanocomposite was somewhat better than that of the I.44P.

The I.44P modifier has two long alkyl tails whereas the C25A pillaring agent has only a single long chain. A previous investigation of nylon 6/alkylammonium-modified clay exfoliation [29] showed that the presence of two alkyl tails sterically diminishes the nylon's ability to interact with the silicate surface and increases the magnitude of the polar nylon/hydrophobic hydrocarbon interaction. A similar observation was also made for poly(lauryl lactam)-adipic acid-poly(tetramethylene ether) glycol block copolymer/C25A and poly(lauryl lactam)-adipic acid-poly(tetramethylene ether) glycol

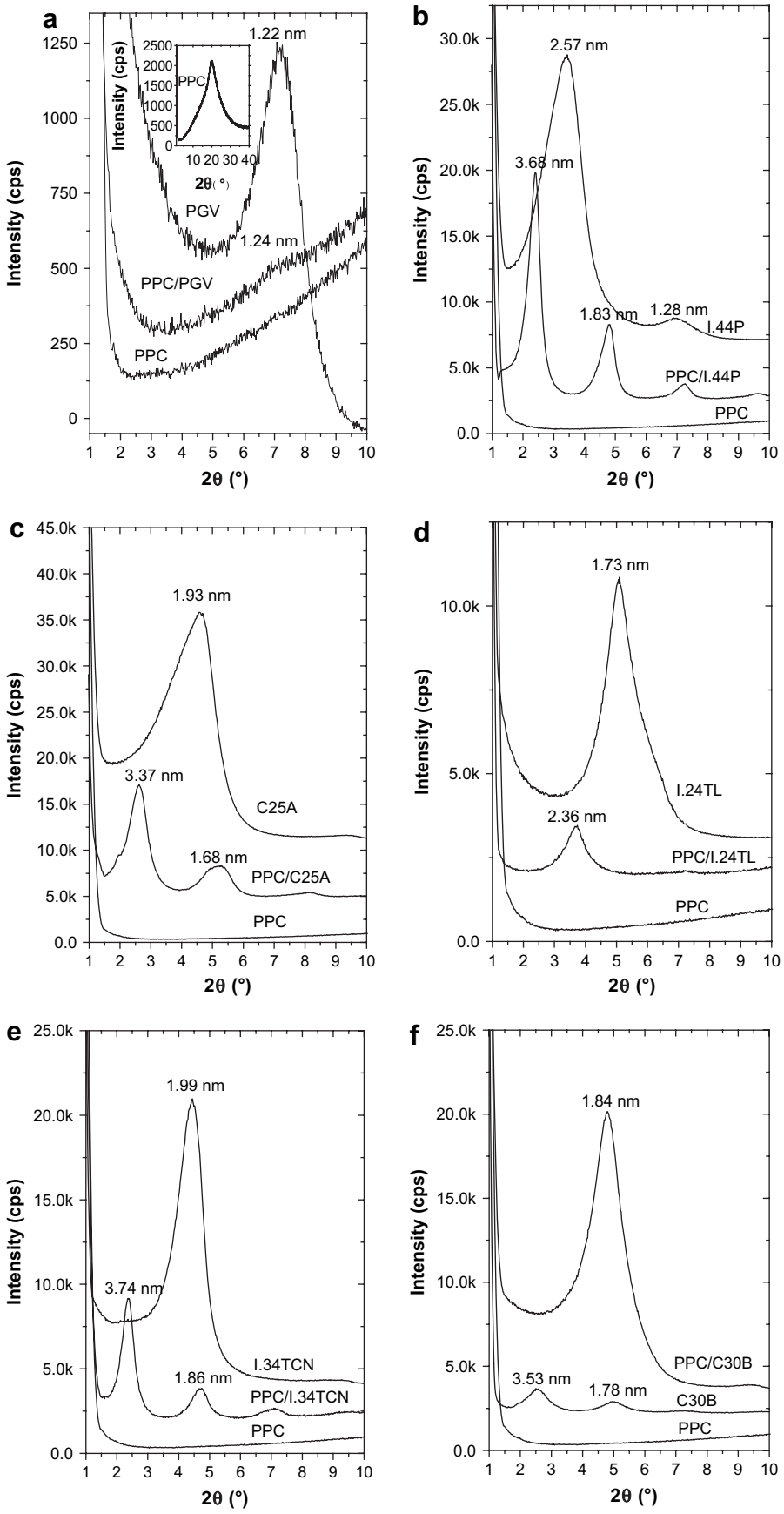

Fig. 2. XRD patterns of (a) PPC, PGV and the PPC/PGV composite, (b) PPC, I.44P and the PPC/I.44P nanocomposite, (c) PPC, C25A and the PPC/C25A nanocomposite, (d) PPC, I.24TL and the PPC/I.24TL nanocomposite, (e) PPC, I.34TCN and the PPC/I.34TCN nanocomposite, and (f) PPC, C30B and the PPC/C30B nanocomposite. All clay loadings are 2.5 wt%.

Table 3
XRD analyses of the clays and PPC/2.5 wt% clay composites[a]

Clay	Pristine clay		Composite		Clay to composite variation	
	d^0_{001} (nm)	I^0_{001} (cps)	d_{001} (nm)	I_{001} (cps)	$\Delta d_{001}/d^0_{001}$ (%)	$-\Delta I_{001}/I^0_{001}$ (%)
PGV	1.22	–	1.24	–	1.61	–
I.44P	2.57	21776	3.68	17850	43.19	18.03
C25A	1.93	24815	3.37	12902	74.61	48.01
I.24TL	1.73	7860	2.36	1958	36.42	75.09
I.34TCN	1.99	16965	3.74	7668	87.93	54.78
C30B	1.84	16660	3.53	1679	91.85	89.92

[a] *I* stands for the peak intensity. The superscript 0 refers to the *d*-spacings and intensities of the starting clays.

block copolymer/Cloisite 15A nanocomposites [30]. This is also likely to occur for the polar PPC.

The d_{001} spacing of PPC/I.24TL increased to 2.36 nm from 1.73 nm in the starting I.24TL clay and no other peaks were apparent (Fig. 2d). The PPC/I.24TL nanocomposite had the second largest $-\Delta I_{001}/I^0_{001}$ value and the smallest $\Delta d_{001}/d^0_{001}$ value among all the nanocomposites. The carboxyl groups of the linear 12-aminododecanoic acid, e.g. pillaring agent **2** in I.24TL and the PPC carbon carbonyl groups should interact by H-bonding and dipole attraction. The XRD (and TEM) findings for the PPC/I.24TL nanocomposite also indicated an intercalated morphology. Since PPC contains a hydroxyl group at one chain end, these functions may esterify the carboxyl group of 12-aminododecanoic acid during the 160 °C blending step, binding some PPC to the clay platelets through the pillaring agent spacer.

The $\Delta d_{001}/d^0_{001}$ values for the PPC/C30B and PPC/I.34TCN nanocomposites were the highest and second highest, respectively, in the series, while their $-\Delta I_{001}/I^0_{001}$ values were the first and third, respectively. This implies that these organoclays should exhibit better degrees of dispersion in the nanocomposites. This is consistent with the development of hydrogen bonding between the pillaring agents' hydroxyl groups (in the $-CH_2CH_2OH$ functions) of these two clays and the PPC's carbonyl groups.

The degree of clay dispersion in these PPC nanocomposites predicted by the XRD analyses followed the order: C30B > I.34TCN and these were followed by C25A > I.44P ≫ PGV. The position of I.24TL in this series was not obvious and had to be determined by TEM.

3.3. Transmission electron microscopy

TEM was used to determine the effect of the clay pillaring agents on the clay platelet dispersion in PPC (Fig. 3). Large PGV aluminasilicate particles and tactoids which remained agglomerated (Fig. 3a) were observed in PPC/PGV samples, confirming very poor nanodispersion. The PPC chains could not be readily inserted into the inorganic PGV platelet galleries. Thus, *d*-spacing expansion, intercalation and exfoliation processes did not easily occur to promote nanodispersion. In contrast, PPC chains were progressively intercalated into the galleries of organoclay I.44P tactoids (Fig. 3b). Furthermore, the TEM of PPC/I.44P nanocomposite also showed that some 'particles' and aggregates were present with diameters between 0.7 and 1.5 μm, ranging in thickness from ~200 to ~50 nm. Organoclay C25A separated into long tactoids with thicknesses ranging from about 30 to approximately 150 nm (Fig. 3c) when blended into the PPC. Clay I.24TL was dispersed into long tactoids which were thinner on average (all observed were less than 100 nm thick) than those from C25A (Fig. 3d). The linear 12-aminododecanoic acid pillaring agent in I.24TL interacted, or possibly reacted, with the PPC to connect some macromolecular chains to the platelets. If this occurred at two positions on a single intercalated PPC polymer molecule with 12-aminododecanoic acid pillars located on adjacent I.24TL platelets, these two platelets could become bonded together through PPC in the PPC/I.24TL nanocomposite.

Organoclay I.34TCN was dispersed in PPC in the form of shorter and thinner average sized tactoids than I.24TL tactoids (Fig. 3e). The C30B was separated into somewhat thinner and shorter tactoids in its nanocomposite than I.34TCN (Fig. 3f). Therefore, the PPC/C30B and PPC/I.34TCN nanocomposites were both partially exfoliated and also contained small amounts of intercalated structures. The highest degrees of nanodispersion in PPC occurred using either C30B or I.34TCN. Similarly, a maleated end-capped PPC/C30B nanocomposite was reported [20] to have a partially delaminated structure. However, the carboxyl groups of the maleated end-capped PPC reacted with the hydroxyl groups of the C30B pillars. Therefore, more PPC-MA was tethered to the C30B platelet surfaces [20]. Consequently, C30B had a higher level of delamination and a better degree of dispersion in PPC-MA nanocomposite than in PPC nanocomposite.

Examination of many TEM images confirmed that the degree of clay dispersion in the PPC composites followed the order: C30B ≈ I.34TCN > C25A ≈ I.24TL > I.44P ≫ PGV. Composites with C30B or I.34TCN were obviously the most highly nanodispersed and these were the two with the smallest $\Delta\delta$ values (solubility parameter difference between their pillaring agents versus PPC, 3.64 and 3.62, respectively, see Table 1). Clay C25A, I.24TL and I.44P with the greater pillaring agent versus PPC $\Delta\delta$ values (6.66–6.16) were less well dispersed.

3.4. Thermogravimetric analysis

The TGA and DTG curves of the PPC and PPC/clay composites are shown in Fig. 4. Table 4 summarizes the 5%, 10% and 50% weight loss decomposition temperatures of these composites, defined as $T_{d,5\%}$, $T_{d,10\%}$ and $T_{d,50\%}$, respectively, obtained under nitrogen at a 10 °C/min heating rate. Table 4 also lists the maximum decomposition rate temperatures, $T_{max,d}$, observed at these conditions for the PPC and PPC/clay composites. The corresponding $T_{d,5\%}$ and $T_{d,10\%}$ values for the starting as-received clays, obtained from TGA curves in Fig. 5, appear in Table 5 for comparison.

The presence of dispersed organoclays within the PPC caused a notable 30–40 °C increase of the PPC's thermal stability (Table 4). However, unmodified PGV clay did not enhance PPC's thermal stability. It was very poorly dispersed. In contrast, the PPC/I.24TL nanocomposite had the highest thermal stability. As seen in Table 4, the $T_{d,5\%}$, $T_{d,10\%}$, $T_{d,50\%}$ and $T_{max,d}$ values of the PPC/I.24TL nanocomposite were 37.8, 42.7, 55.8 and 62.3 °C higher than those of molten PPC. This clearly illustrates the importance of large clay/polymer surface contact areas. Intercalated or partially exfoliated silicate platelets reduce segmental motions of PPC at the PPC/clay interface and to some degree in the nearby interphase region, reducing the chain degradation rate. Nanodispersion generates large platelet/polymer surface interfacial areas and significant interphase volume fractions. Other cases of nanoclays increasing polymer thermal stability have been reported [31–33]. The increases of $T_{d,5\%}$ and $T_{max,d}$ (Table 4) were markedly larger than those of the PPC/C20A nanocomposites reported by Xu et al. [19].

The $T_{d,5\%}$, $T_{d,10\%}$, $T_{d,50\%}$ and $T_{max,d}$ values of PPC/PGV composite were actually a little lower than those of pristine PPC. This occurs because the PGV particles did not become extensively nanodispersed and the PPC present at the surfaces represented a minor fraction of all PPC in the composite. The order of composite thermal stabilities was I.24TL > I.34TCN > C30B > I.44P > C25A > PGV. This order is near to that of the predicted miscibilities except for the PPC/I.24TL nanocomposite. The degrees of dispersion of organoclays I.34TCN and C30B were high, consistent with a higher fraction

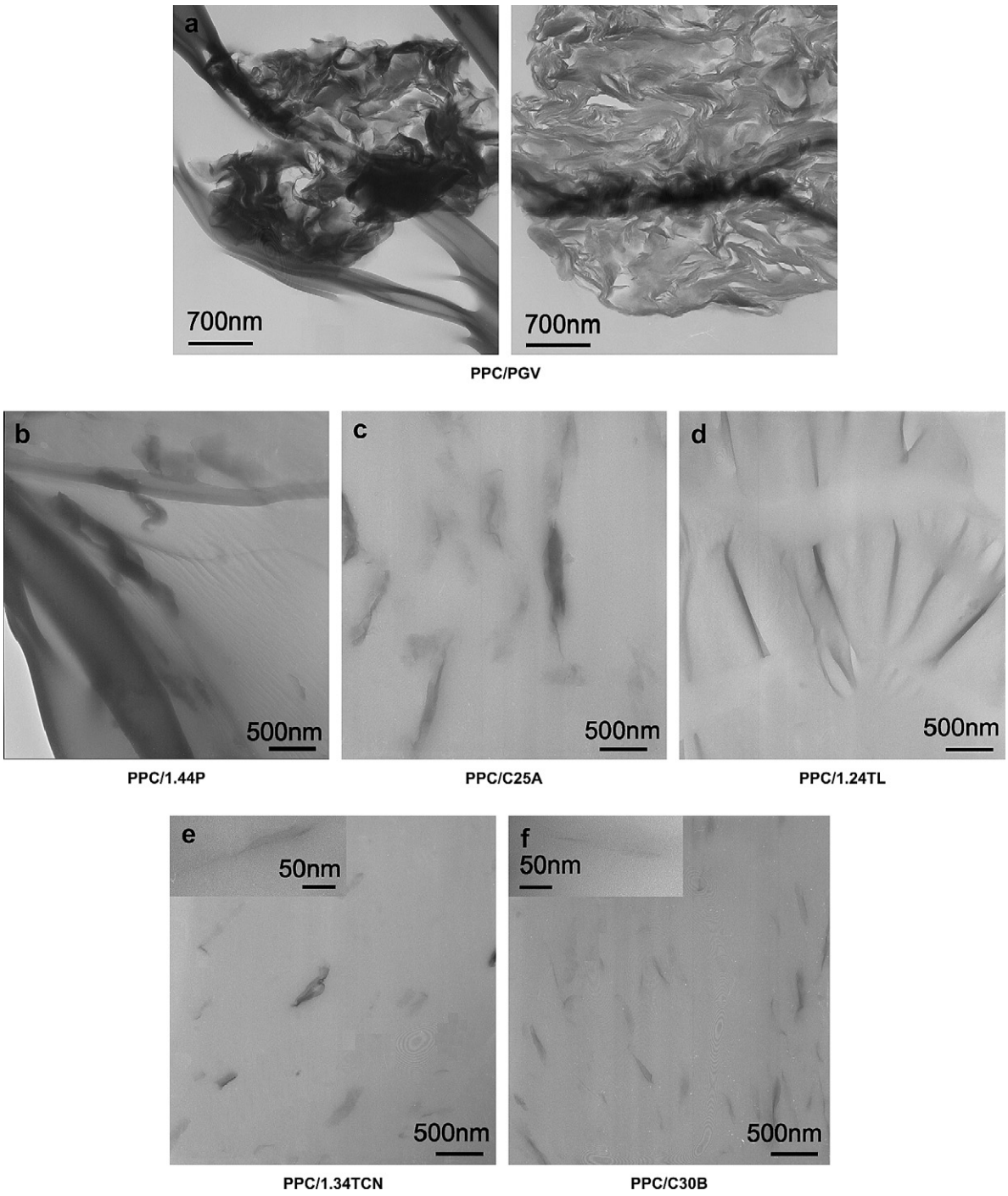

Fig. 3. TEM images of (a) PPC/PGV composite, (b) PPC/I.44P nanocomposite, (c) PPC/C25A nanocomposite, (d) PPC/I.24TL nanocomposite, (e) PPC/I.34TCN nanocomposite and (f) PPC/C30B nanocomposite. All clay loadings were 2.5 wt%.

of all PPC molecules lying at or near the clay surface. The PPC/I.24TL nanocomposite had the highest nanocomposite thermal stability, but I.24TL only ranked as the third or fourth most highly nanodispersed clay in PPC based on XRD and TEM analyses.

The 12-aminododecanoic acid pillaring agent **2** in I.24TL was the most stable of the modifiers used as indicated by comparing the $T_{d,5\%}$ and $T_{d,10\%}$ values of the pure organoclays (Table 5). The primary ammonium pillar is chemically more stable to elimination reactions than the quaternary ammonium pillars. The other pillaring agents had thermal stabilities similar to each other but lower than 12-aminododecanoic acid. The more miscible PPC/I.34TCN and PPC/C30B nanocomposites had higher thermal stabilities than the less miscible PPC/I.44P and PPC/C25A nanocomposites, as measured by TGA. However, only nanocomposite PPC/I.24TL exhibited an obviously higher thermal stability than the others. The key point to emphasize was the marked increase of the PPC/organoclay thermal stabilities versus that of PPC/PGV at equal clay loadings. This shows that both surface area and organoclay's thermal stability are important.

Fig. 5 displays the TGA curves for the pristine PPC and the as-received organoclays. Their thermal stabilities are listed in Table 5. The organoclays exhibited 5% weight losses at temperatures from

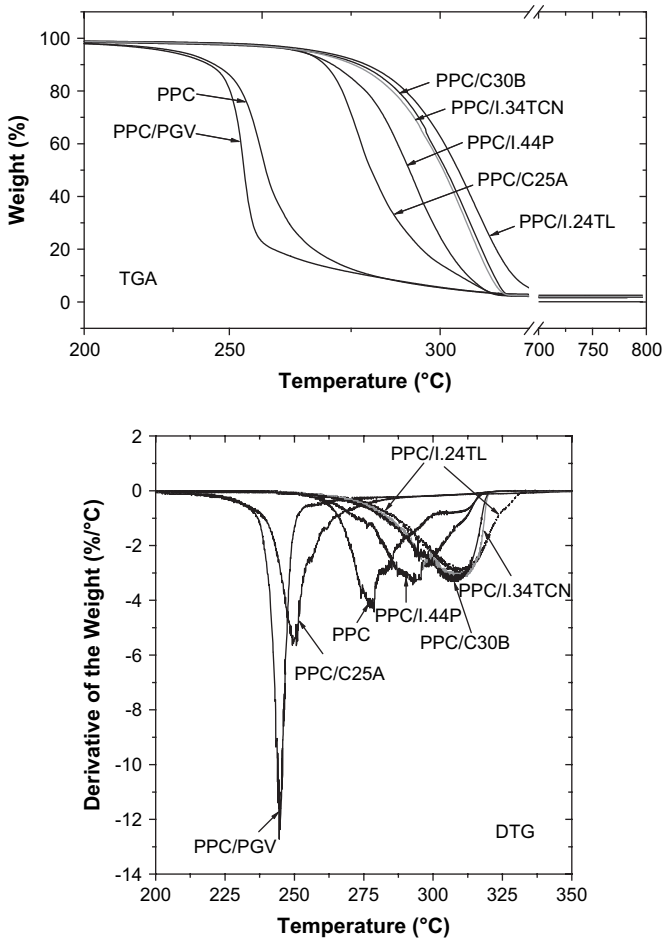

Fig. 4. TGA and DTG curves of the PPC and PPC/2.5 wt% clay composites obtained at a 10 °C/min heating rate under nitrogen. No further changes observed up to 800 °C.

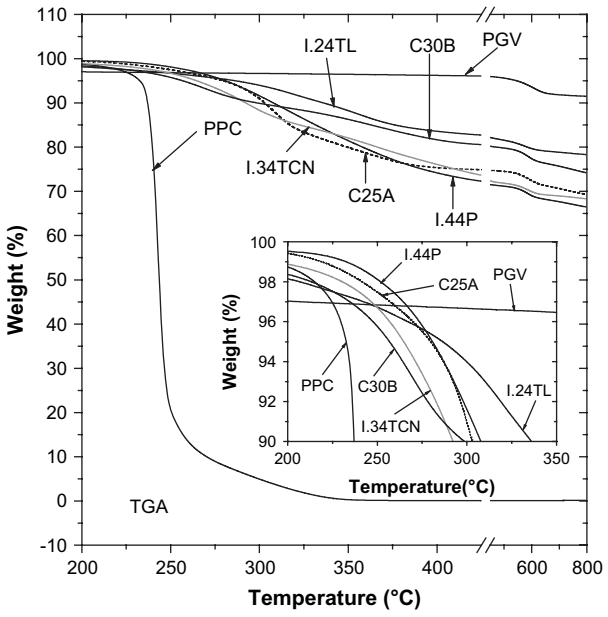

Fig. 5. TGA curves obtained from the pristine PPC and the as-received clays.

Table 5
Thermal stabilities of the pristine PPC and the as-received organoclays

Sample	$T_{d,5\%}$ (°C)	$T_{d,10\%}$ (°C)
PPC[a]	232.6	237.1
PGV	546.0	>800.0
I.44P	280.8	307.8
C25A	279.1	302.9
I.24TL	286.5	336.0
I.34TCN	264.7	292.3
C30B	256.8	298.6

[a] As-received PPC, which had been vacuum dried but not melt processed, was used here. This accounts for the difference in $T_{d,5\%}$ and $T_{d,10\%}$ values for PPC here versus those in Table 4.

a low of 256 °C to a high of 286 °C. This reflects the temperature where Hoffmann elimination occurs from the pillaring agents. The $T_{d,5\%}$ and $T_{d,10\%}$ values in Table 5 demonstrated the following order of organoclay thermal stabilities: I.24TL > I.44P > C25A > I.34TCN ≈ C30B. Within this relatively narrow stability range, only the I.24TL stands out as appreciably more thermally stable. Similar behavior was previously found for poly(glycidylmethacrylate-*co*-methylmethacrylate)-cyclohexanedicarboxylic anhydride/montmorillonite nanocomposite with hexadecyltributylphosphonium cation serving as the modifier [34]. I.24TL contains a pillaring agent with a primary ammonium ion, $^{-}OOC(CH_2)_{10}CH_2NH_3^{+}$, that is more resistant to Hoffmann elimination than quaternary ammonium species. C30B and I.34TCN, which contain 2-hydroxyethyl groups in their pillaring agents, had the lowest thermal stability ($T_{d,5\%}$ and $T_{d,10\%}$ values) among the various clays (Table 5) but they were the most highly nanodispersed. This implies that the slightly better thermal stabilities of the PPC/C30 and PPC/I.34TCN nanocomposites versus those of the nanocomposites containing clays I.44P and C25A resulted mainly from the excellent dispersion of these two partially exfoliated organoclays. The PPC/organoclay's $T_{d,5\%}$ values probably reflect a larger component of the pillaring agents' decompositions versus PPC's decomposition within this small 5% weight loss range. Since the total amount of pillaring agent is less than 1 wt% of the total weight of the composite, the PPC/organoclays' $T_{d,50\%}$ values are due almost entirely to PPC's decomposition. These values show that clays I.24TL, I.34TCN and C30B best stabilized PPC to thermal decomposition. This agrees with TEM analyses which show these are the more highly nanodispersed clays within the series studied.

Table 4
Thermal stabilities of the molten PPC and PPC/2.5 wt% clay composites under nitrogen[a]

Sample	$T_{d,5\%}$ (°C)	$T_{d,10\%}$ (°C)	$T_{d,50\%}$ (°C)	$T_{max,\,d}$[b] (°C)	Char yield (%) at 800 °C
PPC[c]	228.4 ± 1.4	237.0 ± 0.9	250.1 ± 1.1	249.9 ± 0.6	0.12 ± 0.02
PGV[d]	225.0 ± 1.2	235.2 ± 0.6	244.4 ± 0.8	244.3 ± 0.8	2.44 ± 0.13
I.44P[d]	260.6 ± 0.8	270.0 ± 0.6	291.6 ± 0.5	293.6 ± 0.2	1.71 ± 0.09
C25A[d]	260.5 ± 0.5	267.5 ± 0.3	282.0 ± 1.1	277.3 ± 0.2	1.96 ± 0.13
I.24TL[d]	266.2 ± 0.1	279.7 ± 0.3	305.9 ± 0.5	312.2 ± 0.5	1.97 ± 0.15
I.34TCN[d]	263.9 ± 0.6	277.1 ± 0.5	300.4 ± 1.5	304.6 ± 1.3	1.83 ± 0.06
C30B[d]	262.3 ± 0.6	275.2 ± 0.4	300.0 ± 0.6	309.2 ± 0.2	1.96 ± 0.02

[a] The average values of three independent measurements. The ± values specify the absolute value of the difference between each measured value and the average value, averaged over all three measurements. A heating rate of 10 °C/min was applied.
[b] The temperature at which the maximum rate of decomposition (weight loss) occurred under these conditions.
[c] This PPC sample had been melt processed in the Haake Rheomix 600 mixer at 160 °C for 12 min. These are the same conditions used for the preparation of each of the PPC/clay composites. Any molecular weight distribution changes due to high shear at 160 °C should be the same in both the neat PPC and the composites.
[d] Values are for the PPC composites prepared from the clays listed in this column where the clay loading in all cases was 2.5 wt%.

3.5. Rheology

The dynamic amplitude sweeps of the PPC and PPC/clay composites are displayed in Fig. 6. In this figure, the shear storage

moduli, G', shear loss moduli G'', and complex viscosities $|\eta^*|$, respectively, are plotted versus the applied shear strain, γ, at a 1 rad/s frequency in plots (a)–(c). All the samples exhibited linear viscoelastic behavior within a strain range of 1%. PPC had more extensive linear viscoelastic zones up to the critical shear strain, γ_c, values. PPC's γ_c values were 87.3% for G', G'', and $|\eta^*|$. The PPC/PGV composite had slightly narrower linear ranges than the PPC. The γ_c values for the PPC/PGV composite were 65.8% for both G' and $|\eta^*|$ and 57.1% for G''. In contrast, PPC/organoclay nanocomposites had much narrower linear ranges, especially for the PPC/C25A and PPC/I.44P nanocomposites. They exhibited the smallest and second smallest critical shear strain, γ_c, values of 16.0% and 10.5% for G', 66.7% and 50.2% for both G'' and $|\eta^*|$, respectively. Similar observations were made previously for poly(lauryl lactam)-adipic acid-poly(tetramethylene ether) glycol block copolymer/organoclay nanocomposites [30] and a polypropylene/4.8 wt% clay/maleated polypropylene nanocomposite [35].

The G', G'' and $|\eta^*|$ values of the PPC/PGV composite were higher than those of PPC. However, the PPC/organoclay nanocomposites had even higher G', G'' and $|\eta^*|$ values than either PPC or the PPC/PGV composite. The magnitudes of the G', G'' and $|\eta^*|$ values for the PPC/organoclay nanocomposites followed the order: C30B < I.34TCN < I.44P < I.24TL < C25A. This order was not the same as that of the degree of dispersion for the organoclays in the PPC nanocomposites. The more miscible PPC/I.34TCN and PPC/C30B nanocomposites had smaller G', G'' and $|\eta^*|$ values than the less miscible PPC/I.24TL, PPC/I.44P and PPC/C25A nanocomposites. One possible explanation is that the hydroxyl groups of both **3** (in I.34TCN) and **5** (in C30B) could absorb and tightly bind some water in the clay galleries. This moisture could hydrolytically cleave PPC at the carbonate carbonyl groups quite easily at higher rheology temperatures and alternating shear stresses. Both clays C30B and I.34TCN were also nanodispersed very well. This would aid PPC cleavage by water during high shear blending at 160 °C. If enough PPC cleavage occurred, this could lower the G', G'' and $|\eta^*|$ values of the nanocomposites.

Fig. 7 shows the dynamic frequency sweeps of the PPC and PPC/clay composites from 0.05 to 100 rad/s at 1% strain within the linear viscoelastic zones. The G' and G'' values of the PPC/PGV composite (Fig. 7a and b) were higher than those of PPC. The PPC/organoclay nanocomposites had higher G' and G'' values than either the PPC or the PPC/PGV composite. These differences (in Fig. 7a and b) became more apparent in the plots at lower frequencies but the G' and G'' axes are logarithmic so that the absolute differences in G' and G'' magnitudes at high frequencies are significant (Table 6). The organoclay nanocomposites had smaller terminal slopes in the G' and G'' versus ω curves than either the PPC/PGV composite or the PPC. This corresponds to changes from more viscous liquid-like behaviors for both the PPC and the PPC/PGV composite to more elastic solid-like behaviors for all the PPC/organoclay nanocomposites [12,36].

PPC revealed $G' < G''$ when $\omega < 56.9$ rad/s, and $G' > G''$ when $\omega > 68.7$ rad/s (Fig. 7c). Thus, PPC exhibited a liquid-like behavior when $\omega < 56.9$ rad/s. The G' and G'' crossover for the PPC/PGV composite shifted to a lower frequency range (32.4–39.1 rad/s) versus that for PPC. The crossover values for the PPC/organoclay nanocomposites shifted to even lower frequency ranges. This implies that the solid-like behavior ranges are wider and exist at lower frequencies for the organoclay nanocomposites [37–39].

PPC and the PPC/PGV composite exhibited similar Newtonian $|\eta^*|$ versus ω behaviors in the low frequency zones (Fig. 7d). They became shear thinning in the high frequency zones. The PPC/PGV

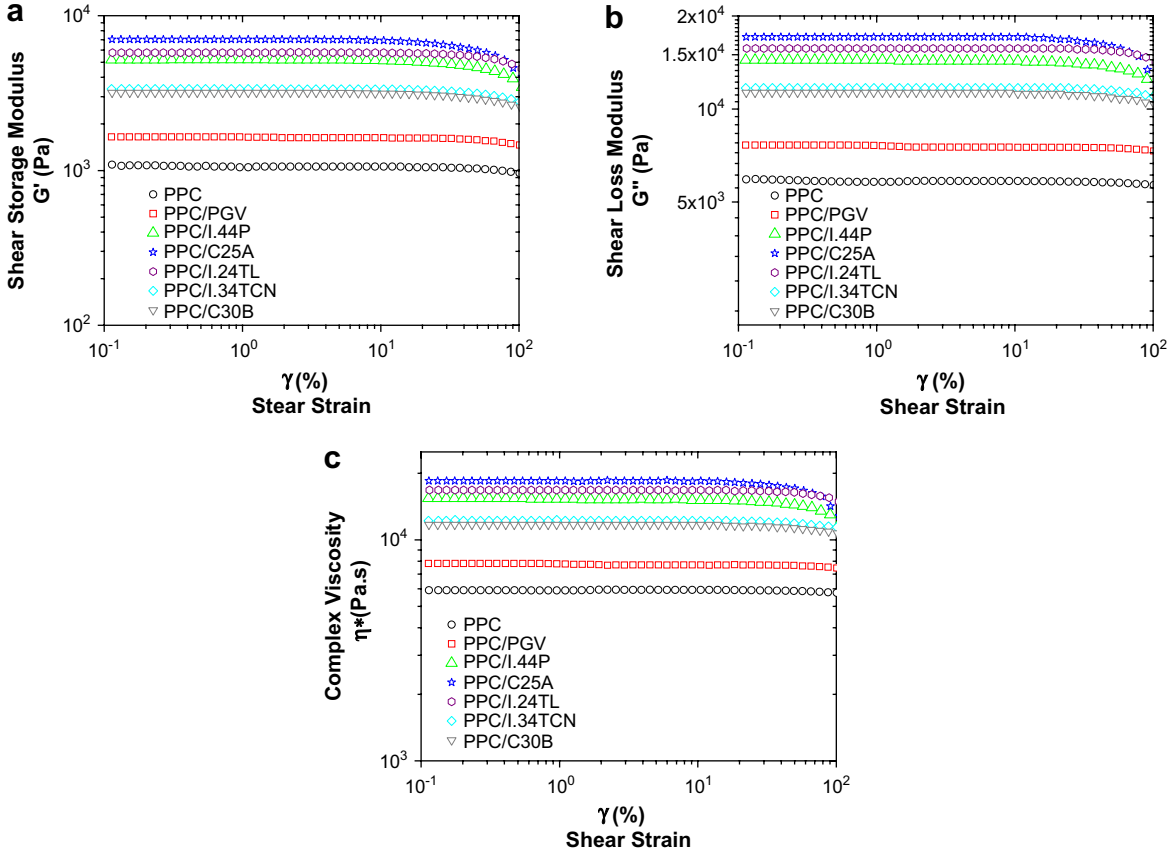

Fig. 6. Dynamic amplitude sweeps of the PPC and PPC/clay composites from 0.1 to 100% strains at a 1 rad/s frequency. (a) G', (b) G'' and (c) $|\eta^*|$.

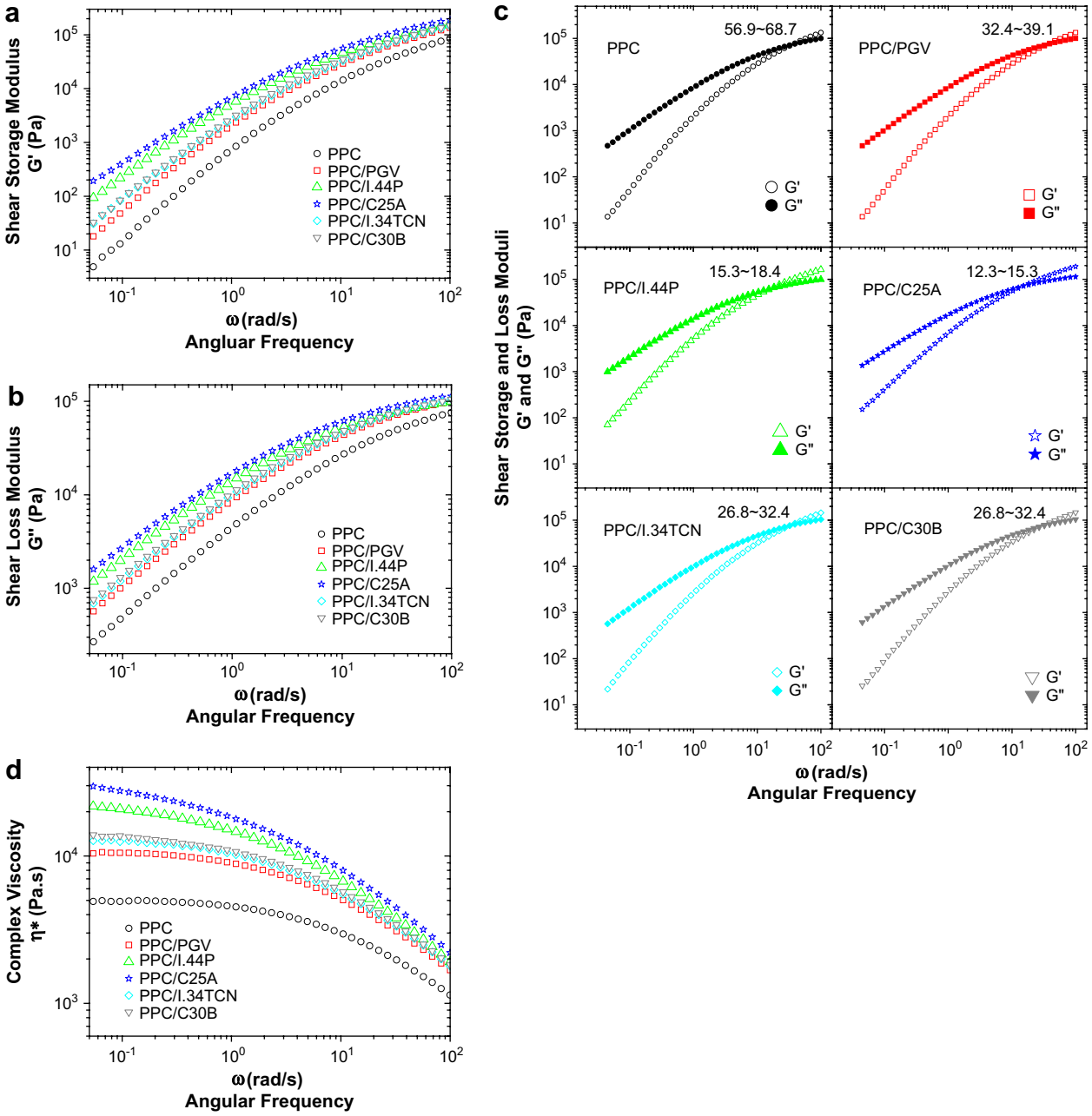

Fig. 7. Dynamic frequency sweeps of the PPC and PPC/clay composites at frequencies from 0.05 to 100 rad/s at 1% strains. (a) G', (b) G'', (c) G' and G'' and (d) $|\eta^*|$.

composite had a higher $|\eta^*|$ value than PPC. In comparison, the PPC/organoclay nanocomposites displayed more pronounced shear thinning and much greater $|\eta^*|$ values in the lower frequency zones. This agrees with the better degrees of organoclay dispersion in these nanocomposites. The PPC nanocomposites containing I.34TCN and C30B had lower $|\eta^*|$ values than the PPC/C25A

Table 6
The G' and G'' values at various angular frequencies, ω, of PPC and PPC/clay composites

	ω [rad/s]	PPC	PPC/PGV	PPC/I.44	PPC/C25A	PPC/I.34TCN	PPC/C30B
G'	100	8.56×10^4	1.35×10^5	1.63×10^5	1.90×10^5	1.45×10^5	1.48×10^5
	10.5	1.45×10^4	2.92×10^4	4.64×10^4	5.62×10^4	3.31×10^4	3.50×10^4
	1.10	8.47×10^2	2.36×10^3	5.78×10^3	7.55×10^3	2.99×10^3	3.20×10^3
	0.115	1.85×10^1	6.68×10^1	2.86×10^2	4.89×10^2	1.11×10^2	1.16×10^2
	0.045	4.39×10^0	1.38×10^1	7.02×10^1	1.52×10^2	2.20×10^1	2.57×10^1
G''	100	7.58×10^4	1.00×10^5	9.96×10^4	1.13×10^5	1.05×10^5	1.05×10^5
	10.5	2.74×10^4	4.38×10^4	5.31×10^4	6.19×10^4	4.73×10^4	4.85×10^4
	1.10	4.89×10^3	9.43×10^3	1.50×10^4	1.81×10^4	1.08×10^4	1.13×10^4
	0.115	5.69×10^2	1.20×10^3	2.34×10^3	3.08×10^3	1.45×10^3	1.55×10^3
	0.045	2.24×10^2	4.71×10^2	9.84×10^2	1.35×10^3	5.71×10^2	6.13×10^2

nanocomposite. These trends were also found in two types of thermoplastic polyurethane matrices including 4,4′-diphenylmethane diisocyanate-based hard block and poly(tetramethylene oxide)-based soft block nanocomposites containing the organoclays C30B or C25A [40].

4. Conclusions

PPC/organoclay nanocomposites were prepared via high shear melt-compounding. The solubility parameter values, δ, of the polymer PPC and the pillaring agents **1**–**5** (Fig. 1) were calculated using group contribution methods of Van Krevelen. Previous δ values of **4** and **5** from the literature [23,24] were somewhat different from those calculated in our work due to different assumptions made. The predicted miscibilities of PPC with the organoclays were obtained from the $|\delta_{PPC} - \delta_{modifier}|$ values.

XRD and TEM both showed that the PPC/PGV composite was an immiscible composite (e.g. PGV was not nanodispersed). The PPC/I.44P, PPC/C25A and PPC/I.24TL nanocomposites had intercalated structures and I.34TCN and C30B were more highly nanodispersed with partially exfoliated morphologies in the PPC. The degrees of dispersion of the clays in the PPC were in the following order: C30B $\approx$ I.34TCN > C25A $\approx$ I.24TL > I.44P $\gg$ PGV. The pillaring agents in C30B and I.34TCN had the smallest $|\delta_{PPC} - \delta_{modifier}|$ values, predicting higher miscibilities with PPC and higher degrees of nanodispersion as observed.

Inorganic clay, PGV, slightly deteriorated the thermal stability of PPC, whereas the organoclays markedly raised the thermal stability. The thermal stability of the PPC/I.24TL nanocomposite is related to the thermal stability of the clay I.24TL's pillaring agent, $^{-}OOC(CH_2)_{10}CH_2NH_3^+$, which contains a primary ammonium ion. Nanocomposite's thermal stability is also related to improved degrees of clay nanodispersion as exemplified by the partially exfoliated morphologies of PPC/I.34TCN and PPC/C30B.

The first rheological studies of the PPC/organoclay nanocomposites were conducted, demonstrating that the PPC/organoclay nanocomposites had the narrower linear viscoelastic zones than either the PPC or the PPC/PGV composite. In the linear viscoelastic zones, the PPC/organoclay nanocomposites showed higher G', G'', and $|\eta^*|$ values and greater levels of shear thinning than the PPC/PGV or PPC. The G' and G'' crossover values for PPC/organoclay nanocomposites were shifted to lower frequencies. Therefore, all the PPC/organoclay nanocomposites exhibited more elastic solid-like behaviors, consistent with the better organoclay dispersion. Moreover, the shear storage modulus, shear loss modulus and complex viscosity values of the more miscible PPC/I.34TCN and PPC/C30B nanocomposites were smaller than those of the less miscible PPC/organoclay nanocomposites even though the dispersion degrees of I.34TCN and C30B in the nanocomposite were better. Perhaps this occurs because the PPC's resistance to hydrolytic cleavage was worse and the I.34TCN and C30B hydrophilicities were better, leading to some lowering of PPC's molecular weight.

Acknowledgements

This research was supported by the 2nd Phase BK21 Program funded by Ministry of Education and Human Resources Development of Korea, the Post-doc Program, at the Chonbuk National University of Korea and by the Mississippi State University Education and General Fund. The authors are also grateful for the financial support provided by the Ministry of Commerce, Industry and Energy (MOCIE) and the Korea Industrial Technology Foundation (KOTEF) through the Human Resource Training Project for Regional Innovation.

References

[1] Inoue S, Koinuma H, Tsuruta T. Makromol Chem 1969;130:210–20.
[2] Paddock RL, Nguyen ST. Macromolecules 2005;38:6251–3.
[3] http://www.empowermaterials.com/products/qpac40/.
[4] Hahn RS, Fernstrom PJ, Bhimaraja US, Melody BJ. WO 021,345 A1; 2001.
[5] Gagnon PJ, Jordan DW, Raposa MA, Jossick DJ, Martin GN. US 058,969; 2007.
[6] http://www.empowermaterials.com/applications/binder2.htm.
[7] Wheatley BK, Lundstrom NH, Lynch RD, Scheffee RS, Martin JD. WO 01,034,537 A1; 2001.
[8] Crockett RB, Packer SM, Dixon RL, Anderson NR, Eyre RK, Keshavan MK, et al. US 5,868,885; 1999.
[9] Hwang Y, Ree M, Kim H. Catal Today 2006;115:288–94.
[10] Robins P, Sant'angelo JG. CA 2,508,295 A1; 2006.
[11] Li XH, Meng YZ, Zhu Q, Xu Y, Tjong SC. J Appl Polym Sci 2003;89:3301–8.
[12] Russo GM, Simon GP, Incarnato L. Macromolecules 2006;39:3855–64.
[13] Dong W, Zhang X, Liu Y, Wang Q, Gui H, Gao J, et al. Polymer 2006;47:6874–9.
[14] Wang K, Wang C, Li J, Su J, Zhang Q, Du R, et al. Polymer 2007;48:2144–54.
[15] Yu Z, Yin J, Yan S, Xie Y, Ma J, Chen X. Polymer 2007;48:6439–47.
[16] Mishra JK, Hwang K-J, Ha C-S. Polymer 2005;46:1995–2002.
[17] Mironi-Harpaz I, Narkis M, Siegmann A. Polym Eng Sci 2005;45:174–86.
[18] Hao J, Lu X, Liu S, Lau SK, Chua YC. J Appl Polym Sci 2006;101:1057–64.
[19] Xu J, Li RKY, Meng YZ, Mai Y-W. Mater Res Bull 2006;41:244–52.
[20] Zhang Z, Shi Q, Peng J, Song J, Chen Q, Yang J, et al. Polymer 2006;47:8548–55.
[21] Fuchs O. In: Brandrup J, Immergut EH, editors. Polymer handbook. 3rd ed. New York: John Wiley and Sons; 1989. p. VII/524–6 and Van Krevelen DW. Properties of polymers. Amsterdam, Netherlands: Elsevier Publishers; 1990.
[22] Jang BN, Wang D, Wilkie CA. Macromolecules 2005;38:6533–43.
[23] Krikorian V, Pochan DJ. Chem Mater 2003;15:4317–24.
[24] Ray SS, Bousmina M. Polymer 2005;46:12430–9.
[25] Fornes TD, Yoon PJ, Paul DR. Polymer 2003;44:7545–56.
[26] Morgan AB, Gilman JW, Jackson CL. Proceedings of ACS division of polymeric materials science and engineering, San Francisco, CA, vol. 82. Washington, DC: American Chemical Society; March 2000. p. 270–1.
[27] Morgan AB, Gilman JW. J Appl Polym Sci 2003;87:1329–38.
[28] Lee J-H, Jung D, Hong C-E, Rhee KY, Advani SG. Compos Sci Technol 2005;65:1996–2002.
[29] Fornes TD, Hunter DL, Paul DR. Macromolecules 2004;37:1793–8.
[30] Yang I-K, Tsai P-H. Polymer 2006;47:5131–40.
[31] Huang X, Netravali AN. Biomacromolecules 2006;7:2783–9.
[32] Lee H-T, Lin L-H. Macromolecules 2006;39:6133–41.
[33] Ray SS, Okamoto M. Prog Polym Sci 2003;28:1539–641.
[34] Someya Y, Shibata M. Polymer 2005;46:4891–8.
[35] Solomon MJ, Almusallam AS, Seefeldt KF, Somwangthanaroj A, Varadan P. Macromolecules 2001;34:1864–72.
[36] Gelfer MY, Burger C, Chu B, Hsiao BS, Drozdov AD, Si M, et al. Macromolecules 2005;38:3765–75.
[37] Hyun YH, Lim ST, Choi HJ, Jhon MS. Macromolecules 2001;34:8084–93.
[38] Wooster TJ, Abrol S, MacFarlane DR. Polymer 2005;46:8011–7.
[39] Zhao J, Morgan AB, Harris JD. Polymer 2005;46:8641–60.
[40] Dan CH, Lee MH, Kim YD, Min BH, Kim JH. Polymer 2006;47:6718–30.